# INFLUENCE OF DIFFERENT ALUMINUM CONCENTRATIONS IN CZ-SI WAFERS ON LETID

Melanie Mehler[1], Annika Zuschlag[1], Matthias Trempa[2], Thomas Buck[3], Giso Hahn[1]

[1]University of Konstanz, Department of Physics, 78457 Konstanz, Germany
[2]Fraunhofer-Institute for Integrated Systems and Device Technology, 91058 Erlangen, Germany
[3]International Solar Energy Research Center Konstanz e.V., Rudolf-Diesel-Straße 15, 78467 Konstanz, Germany

ABSTRACT: In this work the influence of different Al concentrations in Cz-Si wafers and the bonding of acceptors with H is investigated. For this purpose, the long-term behavior of the excess charge carrier lifetime is examined for Cz-Si wafers with Al concentrations in the range of ~$10^{13}$-$10^{16}$ $cm^{-3}$. By varying the Al concentration in the Si bulk via changing the doping procedure during crystal growth, samples can be processed containing either more or less Al atoms compared to the overall H concentration in the wafer. At higher Al concentrations in the Si bulk, a significant delay of the degradation and regeneration behavior can be observed. The effect of the Al-induced delay can be shown not only for lifetime samples, but also for PERC solar cells processed from the same Cz-Si material. By using $AlO_x$ passivation layers with varying thickness as a barrier layer for H, the H content in the Si bulk can be reduced after firing of $AlO_x$/$SiN_y$:H stacks. When comparing the lifetime equivalent defect densities $\Delta N_{leq}$ of the $AlO_x$/$SiN_y$:H passivated samples with the $SiN_y$:H passivated samples, a delay in degradation can be observed at higher Al concentrations and low H content in the Si bulk. A possible explanation for the Al-induced delay could be due to the expected stronger binding of H with Al compared to B. From the results of the B-H and Al-H measurements, it can also be suggested that the release of H from the acceptor contributes to the degradation. AlH pairs do not dissolve in the dark like BH. This behavior could also be observed on Ga-doped wafers. The results allow further insights into the origin and kinetics of LeTID.

Keywords: Degradation, Hydrogen, Dopants

## 1 INTRODUCTION

Degradation phenomena such as light and elevated temperature induced degradation (LeTID) can reduce the efficiency of Si solar cells. It could be shown that the strength of LeTID degradation of Cz-Si PERC solar cells correlates with the Al concentration in the Cz wafer [1,2]. Thus, an influence of Al atoms on the LeTID effect can be concluded. The aim in this work is to investigate the impact of Al dopant and its bonding with H on the degradation and regeneration kinetics. For this purpose, complementary to previous work [2], different Al concentrations in the range of ~$10^{13}$-$10^{16}$ $cm^{-3}$ in the Cz-Si wafers are investigated. By using $AlO_x$ layers deposited via atomic layer deposition (ALD) in different thicknesses, which act as a diffusion barrier for H [3], the H content in the Si bulk can be changed. Using Cz-Si wafers differing in Al concentration, samples can be investigated whose H content is higher or lower compared to the Al dopant concentration. This opens up the possibility to study the influence of Al dopants in combination with H-acceptor pair formation on LeTID kinetics.

## 2 EXPERIMENTAL

For the degradation experiments ~1 Ωcm B-doped, two different B+Al co-doped, and ‘pure’ Al doped Cz-Si wafers (referred to as B-Reference, B+Al(1), B+Al(2) and ‘pure’ Al, respectively) serve as base materials. Tab. 1 shows the secondary ion mass spectrometry (SIMS) measurement results of the dopant concentrations for the respective samples.

After the saw damage and a cleaning step, the samples are gettered using a $POCl_3$ diffusion (55 Ω/sq). The resulting emitter is removed in an etching step and the samples are cleaned again. Afterwards, both sides of the samples are deposited with 0-25 nm $AlO_x$ from ALD at 300°C, followed by deposition of 75 nm plasma-enhanced chemical vapor deposition (PECVD) $SiN_y$:H. The samples are fired at $T_{sample,peak}$=810°C and then degraded at 80°C and 0.9(1) suns (same degradation parameters as for the PERC cells). For the measurement under constant injection, the laser setup of [4] was used. The samples were degraded at 220°C and at a constant injection of $\Delta n=1.0\cdot10^{16}$ $cm^{-3}$. The effective minority charge carrier lifetime $\tau_{eff}$ is determined using photoconductance decay (PCD) at 30°C and evaluated at $\Delta n=0.1\ p_0$, with $p_0$ being the doping density. For better comparison of degradation and regeneration behavior from the different samples, the lifetime equivalent defect density $\Delta N_{leq}$ is calculated [5]. For determination of BH and/or AlH pairs via resistivity measurements [6], Al is evaporated on the samples after firing and electrically contacted by LFCs (laser fired contacts). For the formation of acceptor-H pairs, the resistivity samples were treated at 220°C in the dark, and for dissolution at 220°C and 2.2(2) suns. The resistance measurement is performed at 25°C. The process flow for the lifetime and resistivity samples is shown in Fig. 1.

**Table I:** B and Al concentrations in the investigated Cz-Si materials (obtained via SIMS analysis)

| | B conc. [at/$cm^3$] | Al conc. [at/$cm^3$] |
|---|---|---|
| B-Reference | $1.15\text{-}1.2\cdot10^{16}$ | $3\text{-}5\cdot10^{13}$ |
| B+Al(1) | $0.9\text{-}1.1\cdot10^{16}$ | $2.8\text{-}3.4\cdot10^{14}$ |
| B+Al(2) | $0.9\text{-}1.0\cdot10^{16}$ | $4.7\text{-}6.0\cdot10^{15}$ |
| Al | $2.5\text{-}3\cdot10^{13}$ | $1.4\text{-}1.7\cdot10^{16}$ |

The Cz-Si PERC solar cells have been fabricated according to an industrial-type solar cell process from the same base materials. The front side is passivated with silicon nitride $SiN_y$:H and the rear side with silicon oxy-nitride layer $SiO_xN_y$. The solar cell parameters are determined at 25°C using a flasher from H.A.L.M. For a better comparison, the difference $\Delta V_{OC}$ of the measured values to the initial value is considered.

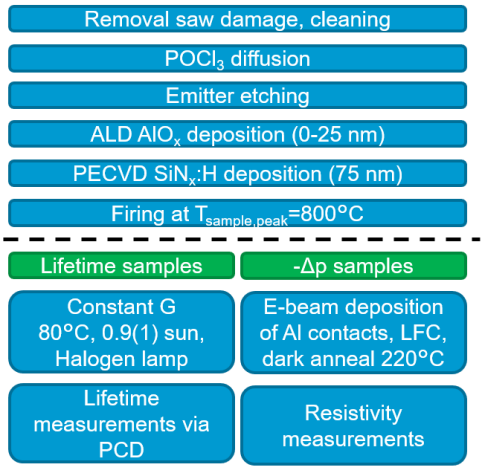


**Figure 1:** Process diagram for the lifetime and resitivity samples.

## 3 RESULTS AND DISCUSSION

Fig. 2 shows the resulting $\tau_{eff}$ and $\Delta N_{leq}$ values for the different samples, passivated with $SiN_y$:H layers only on both sides. Under these degradation conditions, no regeneration occurs for the 'pure' Al sample within 900 h. The initial $\tau_{eff}$ values of the B-Reference and B+Al(1) are comparable, whereas the B+Al(2) and 'pure' Al samples show significantly lower initial $\tau_{eff}$. The reduction in $\tau_{eff}$ at high Al concentrations could be (partly) attributed to Al-O complexes [7].

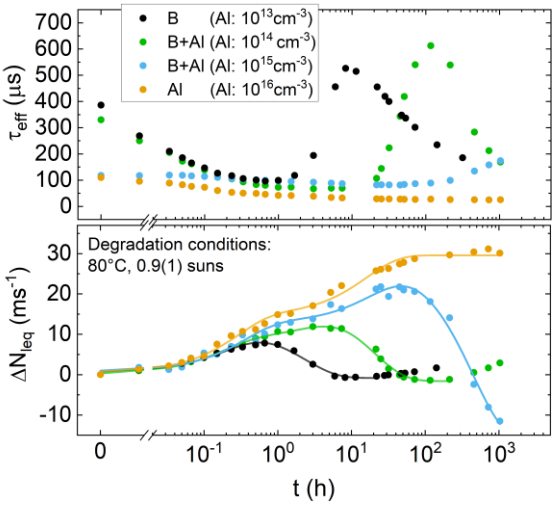


**Figure 2:** $\tau_{eff}$ (top) and $\Delta N_{leq}$ with fit (bottom) over accumulated time for treatment at 80°C, 0.9 suns illumination for the Cz-Si materials with different Al concentrations.

With higher Al concentration, the maximum defect density increases and a delay in degradation and regeneration kinetics is observed. The resulting time constants confirm the delay of degradation and regeneration at higher Al concentrations although the absolute values should be handled with care as injection changes during treatment time. Except for the B-Reference, two exponential functions are used for fitting the degradation. A shoulder can be seen during degradation for the materials B+Al(1), B+Al(2) and 'pure' Al, indicating a two-step degradation. The effect of the Al-induced delay for degradation and regeneration could also be observed at PERC cell level, see Fig. 3.

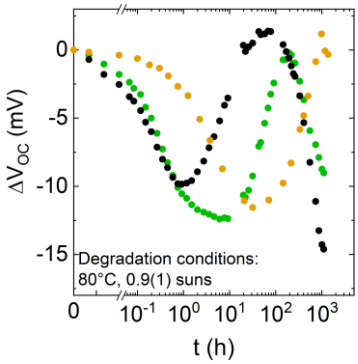


**Figure 3:** $\Delta V_{oc}$ values of the Cz-PERC solar cells over accumulated time for treatment at 80°C, 0.9 suns illumination for the Cz-Si materials with different Al concentrations.

Since $\tau_{eff}$ is different for the various samples, a measurement under constant injection is more reasonable. Fig. 4 shows the resulting $\tau_{eff}$ and $\Delta N_{leq}$ values for the B-Reference, B+Al(1) and 'pure' Al. The degradation temperature was increased to 120°C to analyze the regeneration from 'pure' Al. Also here, a higher Al concentration leads to delayed kinetics. Compared to the measurement with constant illumination, 'pure' Al shows a lower $\Delta N_{leq,max}$ and stronger regeneration compared to the other two materials, maybe indicating that directly after firing a significant amount of LeTID defects is already present. The degradation kinetics have also changed, since only one exponential function is sufficient to fit the degradation. This change in degradation kinetics at constant injection could also be shown in [2].

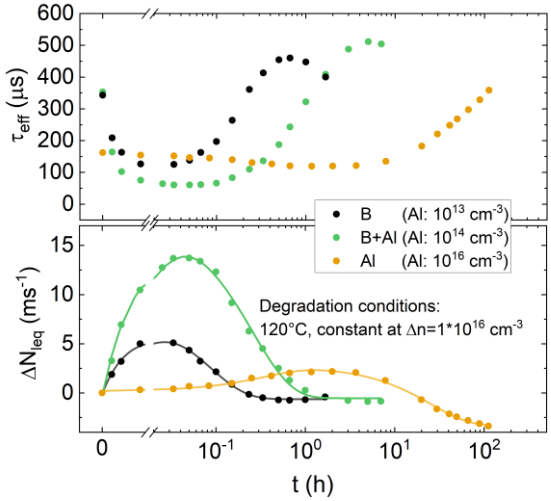


**Figure 4:** $\tau_{eff}$ (top) and $\Delta N_{leq}$ with fit (bottom) over accumulated time for treatment at 120°C and at constant injection for the Cz-Si materials with different Al concentrations.

Fig. 5 shows for the B-Reference, B+Al(1) and 'pure' Al the $\Delta N_{leq}$ values for the samples passivated with ALD $AlO_x$ / PECVD $SiN_y$:H followed by firing. The samples in Fig. 5 are from another run but were processed in the same way as the samples shown in Fig. 2 Since the samples were not in the same $SiN_y$:H deposition and not fired on the same day, the $SiN_y$:H passivated samples differ from those

in Fig. 2. As expected, the samples with $AlO_x/SiN_y$:H layers show lower $\Delta N_{leq}$ values than the samples with $SiN_y$:H layer only. For the 'pure' Al sample, the maximum $\Delta N_{leq}$ could be lowered from 20 $ms^{-1}$ to below 5 $ms^{-1}$. Compared to the $SiN_y$:H passivated sample, the degradation time constants of the $AlO_x/SiN_y$:H passivated B+Al(1) samples show comparable values, whereas the Al samples with an additional $AlO_x$ layer show a more significant delay in degradation. Thus, a higher Al concentration and a lower H content in the Si bulk lead to a delay in degradation and regeneration. Again, a shoulder during degradation can be seen in the B+Al(1) samples. A possible explanation for the 2-step degradation in the B+Al(1) material could be that the bonding of H to Al is stronger compared to B, which results in different "release times" of H.

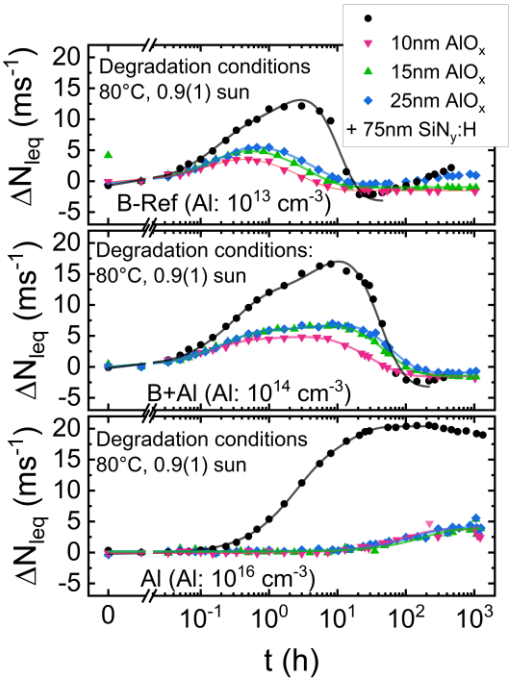


**Figure 5:** $\Delta N_{leq}$ over accumulated time (80°C, 0.9 suns) for samples with $AlO_x$ layers of different thickness plus an additional 75 nm $SiN_y$:H layer for the differently Al doped samples. The data of the B-Reference was already shown in [8].

To explain the delay in degradation and regeneration, the role of H is examined in more detail. Fig. 6 shows for the B-Reference and 'pure' Al the change in hole concentration $-\Delta p$ of the $SiN_y$:H samples. As can be seen, the $-\Delta p$ values show a formation and dissolution of BH pairs. But the pairs do not completely dissolve in the dark, and the resistance can also increase again, for example, due to thermal donors [9]. The degradation temperature for the B-Reference sample is higher compared to Al in order to accelerate the dynamics. In [10] the formation and dissolution of BH pairs between 160-220°C could be shown. In comparison, Al in Fig. 6 shows no dissolution of the AlH pairs at a degradation temperature of 180°C. A similar behavior has also been observed in Ga doped Cz-Si wafers [10].

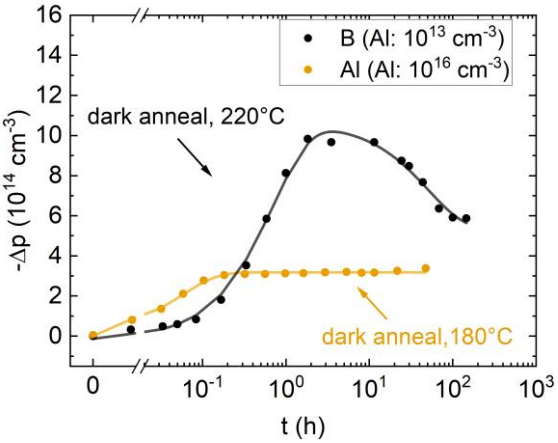


**Figure 6:** $-\Delta p$ over accumulated time for the B-Reference and 'pure' Al samples passivated with 75 nm $SiN_y$:H. The 'pure' Al sample was degraded at 180°C and the B-Reference sample at 220°C in the dark

Assuming that the AlH bond is stronger than the BH bond and the degradation and/or regeneration is also influenced by the dissolution of the acceptor-H complex, this can be an explanation for the observed delayed LeTID kinetics. To resolve the acceptor-H pairs, the samples were treated under light and elevated temperature, analogous to [11]. Fig. 7 shows the formation and dissolution of the acceptor H pairs for the B-Reference and the two B+Al co-doped samples.

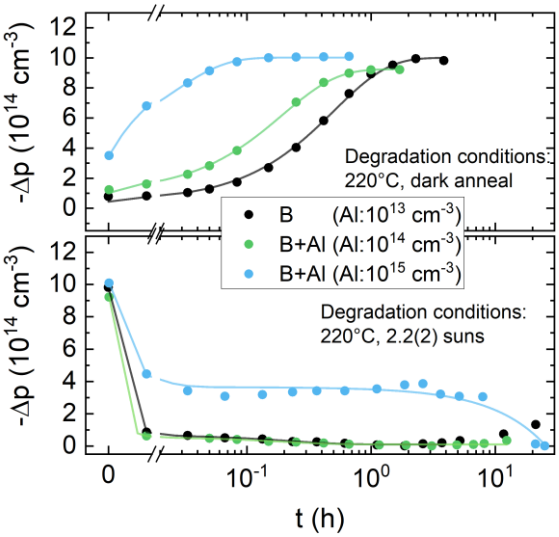


**Figure 7:** $-\Delta p$ over accumulated time for the B-Reference and the two B+Al co-doped samples passivated with 75 nm $SiN_y$:H. For the formation of the acceptor-H pairs, the samples were degraded at 220°C in the dark (top) and for the dissolution at 220°C and 2.2 suns.

The B-Reference and B+Al(1) ([Al]: $10^{14}$ $cm^{-3}$) contain less Al, and B+Al(2) ([Al]: $10^{15}$ $cm^{-3}$) similar or even more Al compared to the overall amount of H. The formation of acceptor-H pairs is faster for the B+Al co-doped samples than for the B reference. The dissolution of the acceptor-H pairs for B+Al(2) ([Al]: $10^{15}$ $cm^{-3}$) proceeds via 2 steps compared to the other samples. Thus, a higher Al concentration seems to accelerate the formation of the acceptor-H pairs and the dissolution of the pairs occurs more slowly.

From the resistance measurements, the initial [$H_2$]

dimers and the concentration of initial acceptor-H pairs can be determined according to [12]. Fig. 8 shows the initial concentrations of the respective species for the B-Reference and the two B+Al co-doped materials. As expected, the concentration of initial acceptor-H pairs increases with higher Al concentration, and the concentration of the initial [$H_2$] dimers decreases. Due to the higher activation energy for the dissolution of AlH-pairs, H dissolves more slowly from Al, which is a possible cause of the delay in LeTID kinetics.

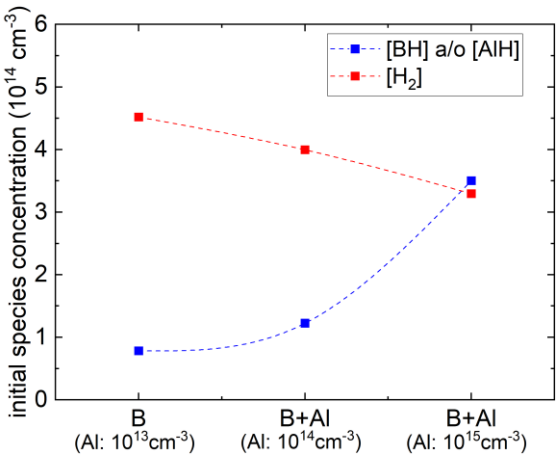


**Figure 8:** Initial concentrations of the acceptor-H pairs and [$H_2$] dimers for the B-Reference and the two B+Al co-doped materials.

## 4 CONCLUSIONS

A higher Al concentration in the Si bulk leads to delayed LeTID degradation and regeneration kinetics. This behavior could be observed under both constant generation and constant injection, as well as on PERC solar cell level.

In addition, using $AlO_x$ barrier layers has shown that higher [Al] and lower [H] leads to delayed kinetics.

Resistance measurements in the dark have shown no dissociation of AlH pairs, unlike for BH pairs. Thus, LeTID degradation and/or regeneration seem to be influenced by the dissociation of acceptor-H pairs. As expected, the B+Al co-doped samples show more initial acceptor-H pairs than the B-Reference. This could be explained by trapping of H at Al, and its release happens more slowly as compared to trapping at B due to the higher activation energy.

## 5 ACKNOWLEDGEMENTS

Part of this work was financially supported by the German Federal Ministry for Economic Affairs and Climate Action (FKZ 03EE1051). The content is the responsibility of the authors.

## 6 REFERENCES

[1] M. Wagner et al., Solar Energy Materials and Solar Cells 187 (2018) 176-188.
[2] M. Mehler et al., Physica Status Solidi A 218(22) (2021) 2100603.
[3] A. Schmid et al., IEEE Journal of Photovoltaics 11(4) (2021) 967-973.
[4] A. Graf et al., AIP Conference Proceedings 2147 (2019) 140003
[5] A. Herguth, IEEE Journal of Photovoltaics 9(5) (2019) 1182-1194.
[6] A. Herguth, C. Winter, IEEE Journal of Photovoltaics 11(4) (2021) 1059-1068.
[7] J. Schmidt et al., IEEE Journal of Photovoltaics 9(6) (2019) 1497-1503.
[8] M. Mehler et al., in Proc. 8th WCPEC, (2022) 142-144.
[9] C. Winter et al., Physica Status Solidi A 218(23) (2021) 2100220.
[10] Y. Acker et al., Physica Status Solidi A 219(17) (2022) 220014.
[11] J. Simon et al., in Proc. 8th WCPEC, (2022) 19-21.
[12] J. Simon et al., Solar Energy Materials and Solar Cells 260 (2023) 112456.